Sensors and Actuators A 265 (2017) 174–180

Contents lists available at ScienceDirect

Sensors and Actuators A: Physical

journal homepage: www.elsevier.com/locate/sna

Spin-Valve based magnetoresistive nanoparticle detector for applications in biosensing

Wenlan Qiu[a,b], Long Chang[b,c], Yu-Chi Liang[d], Julia Litvinov[e], Jing Guo[b], Yi-Ting Chen[f], Binh Vu[d], Katerina Kourentzi[d], Shoujun Xu[f], T. Randall Lee[f], Youli Zu[g], Richard C. Willson[d,b], Dmitri Litvinov[a,b,c,d,f,*]

[a] Materials Science & Engineering, University of Houston, Houston, TX, 77204, USA
[b] Center for Integrated Bio & Nano Systems, University of Houston, Houston, TX, 77204, USA
[c] Department of Electrical & Computer Engineering, University of Houston, Houston, TX, 77204, USA
[d] Department of Chemical & Biomolecular Engineering, University of Houston, Houston, TX, 77204, USA
[e] Department of Internal Medicine, University of Texas Medical Branch, Galveston, TX, 77555, USA
[f] Department of Chemistry, University of Houston, Houston, TX, 77204, USA
[g] Department of Pathology and Genomic Medicine, Houston Methodist Hospital, Houston, TX, 77030, USA

ARTICLE INFO

Article history:
Received 1 June 2017
Received in revised form 27 July 2017
Accepted 7 August 2017
Available online 9 August 2017

Keywords:
Bioinstrumentation
Biosensor
Magnetic particle detection
Magnetoresistive sensors

ABSTRACT

A magnetoresistive sensor platform for the detection of individual magnetic reporter particles is presented. The sensing scheme is based on the detection of the shift in the sensor's magnetoresistance-switching field in the presence of magnetic particle(s). A bottom-pinned spin-valve multilayer (Co/Ru/Co)/Cu/(Co/Ru/Co) device structure (with Ta/Ru seed and Ta capping layers) used for the sensor was deposited using ultra-high vacuum magnetron sputtering and patterned using conventional microfabrication techniques. Inexpensive electronics to measure device magnetoresistance (using DC currents) was used for testing. The detection of individual 500 nm Fe_3O_4 nanoparticles as well as the detection of up to ten (10) nanoparticles was demonstrated and verified using scanning electron microscopy (SEM). The developed sensors are readily integratable into a biosensing platform for the detection of biomolecules at ultra-low concentration using magnetic nanoparticles as reporters.

1. Introduction

Since their first introduction by Baselt et al. in 1998, magnetoresistive (MR) biosensors have been studied as a possible alternative to fluorescent and enzymatic biomarker assays [1–6]. Commercial microarray systems using fluorescent labels require significant amounts of biomolecules to achieve a useful signal-to-noise ratio (SNR) and suffer from issues related to sample turbidity, autofluorescence, and photobleaching [5,7]. MR sensors are compact, inexpensive to manufacture, highly sensitive, and have shown the ability to detect clusters of hundreds down to a few dozens of 16nm–50 nm Fe_3O_4 magnetic nanoparticles (MNPs) using Wheatstone bridge based high precision resistance measurements [7–12].

In a typical spin-valve sandwich structure, two magnetic layers are separated by a nonmagnetic spacer, forming a structure of B/F/NM/F/C, in which B and C designate a buffer/seed and a capping layer, and F and NM are a transition-metal magnetic layer (Fe, Co, Ni or their alloys), and a non-ferromagnetic transition or noble metal (e.g., Cu or, Au), respectively [13]. The overall resistance of such a structure depends on the mutual alignment of the magnetization of the two magnetic layers. When the magnetic layers have parallel magnetization directions, the structure is in its low-resistance state. Antiparallel orientation of the ferromagnetic layers leads to a high-resistance state [13,14]. The ratio of the resistance change between high and low resistance states to the low resistance state, $\Delta R/R = (R_{\uparrow=} - R_{\uparrow\uparrow})/R_{\uparrow\uparrow}$, is a figure of merit of MR sensors because higher $\Delta R/R$ ratios enable higher signal-to-noise ratios (SNRs) for magnetic signal detection. The magnetization of one ferromagnetic layer is typically engineered to be pinned by exchange interaction to an antiferromagnetic layer, while the other layer is designed to rotate its magnetization orientation freely [14]. Magnetic sensors prepared from such spin-valve multilayers often incorporate a built-in biasing magnetic field to improve their switching characteristics and/or enable a linear response to an applied external field.

* Corresponding author at: Electrical & Computer Engineering, University of Houston, Houston, TX, 77204, USA.
E-mail address: litvinov@uh.edu (D. Litvinov).

http://dx.doi.org/10.1016/j.sna.2017.08.018
0924-4247/

Previous work in this area has described relatively large MR biosensors with dimensions on the scale of several micrometers and requiring relatively complex electronics and signal processing (AC-modulated fields, DC bias, and lock-in detection techniques) to achieve the required detection levels [7,10,14–17]. The detected signal is proportional to the coverage of the MNPs on the sensor's surface. To make precise resistance measurements which maximizes the sensitivity of the sensor, a Wheatstone bridge is often used. A full bridge is typically constructed using two MR sensors and two tuning resistors. One MR sensor is biologically active and the other is a reference sensor that is located near the active sensor such that it experiences the same sensing environment such as magnetic fields and temperature. The bridge is balanced by adjusting the tuning resistors. The differential output of the balanced bridge cancels the common mode signal experienced by both the active and reference sensor. If the bridge is not balanced or loses balance due to thermal drift or aging effects, interpretation of the signal is compromised, limiting the practical sensitivity of the device. For example, the temperature coefficients of GMR sensors are approximately 1000 parts per million (PPM)/°C [18] and trim pots are approximately 100 PPM/°C, so a 1° difference in ambient temperature results in a change in resistance that is 90 times larger than the10 PPM change in resistance that is detectable by research instruments.

High sensitivity can be achieved in a different manner by shrinking the size of the MR sensor to approximately the size of a MNP. In contrast to larger MR sensors, in which the entire span of magnetoresistance values is used to count MNPs, such small MR sensors utilize the entire resistance "bandwidth" to detect a single MNP. This quasi-digital approach can enable reliable single particle detection using less precise measurement techniques. In this study, a spin-valve MR sensor is proposed for the detection of individual MNPs. The proposed sensor possesses a small size that helps suppress magnetic domain/switching noise, and can detect individual single MNPs using simple electronics for DC measurements of resistance and a small (<300 Oe) biasing DC field. The sensors are manufactured using established microfabrication techniques and can be integrated into biomolecular assays.

2. Experimental procedure

2.1. Design of spin-valve and detection scheme

In the magnetoresistive spin-valve used in this study, the two magnetic layers are replaced with Co/Ru/Co trilayers for better stability [19] and flexibility [20], where the thickness of the Ru layer is optimized to achieve antiferromagnetic coupling between Co layers. One of the trilayers is designed to be antiferromagnetic and acts as the pinned layer, and the other is designed to be ferromagnetic to switch freely under small magnetic fields. For the pinned layer, Co(5 nm)/Ru/(Co5 nm), the Ru layer thickness is adjusted to achieve antiferromagnetic coupling between the Co layers and saturates at a high field such as above 3000 Oe. The Ru layer thickness for the free layer, Co(5 nm)/Ru/Co(10 nm), is adjusted such that the film switches sharply at a low field such as below 100 Oe. The pinned and free layer is separated by a Cu layer that is thick enough to magnetically decouple them.

The conceived response of the resistance of a bottom-pinned spin-valve sensor in an external magnetic field (R-H loop) is illustrated in Fig. 1. The resistance is low when the magnetization of the free layer aligns with that of the pinned layer. When an applied magnetic field opposing the magnetization of the free layer is sufficiently high, the free layer switches and the spin-valve changes to a high-resistance state. The free layer of the proposed spin-valve structure is optimized to switch as a whole.

The position of the switching field is used to detect the presence of a single MNP in the following manner: As illustrated in Fig. 1, the stray field generated by a MNP placed over the sensor surface is applied in the direction opposite to the direction of the applied external magnetic field, thus effectively reducing the external magnetic field experienced by the sensor. As a result, a higher external field is needed to compensate for the MNP stray field, leading to an increase of the high/low resistance-switching field. This shift of the switching field is used to detect the presence of magnetic particles above the sensor surface. The amount of shift in the switching field is expected to vary with the size, position, and quantity (such as small clusters) of the MNPs, so the output of the sensor signifies only the presence or absence of a stray magnetic field.

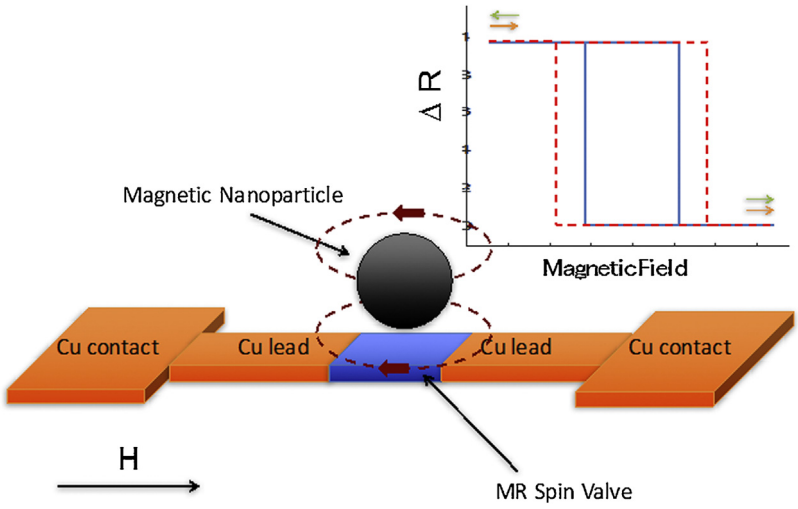

Fig. 1. Schematic illustration of the sensor structure in the presence of one MNP; Inset: Sample ΔR-H loop of a model MR sensor where the blue solid line represents the sensor behavior with no MNP and the red dashed line with the MNP. The arrows represent the directions of magnetization of the free layer (green) and the pinned layer (orange). (For interpretation of the references to colour in this figure legend, the reader is referred to the web version of this article.)

2.2. Sensor fabrication

The spin-valve stack (Ta 2.5 nm/Ru 5 nm/Co 5 nm/Ru 0.8 nm/Co 5 nm/Cu 6 nm/Co 5 nm/Ru 1.4 nm/Co 10 nm/Ta 5 nm) was deposited on oxidized Si wafers (500 nm SiO_2) using an AJA ATC 2200 ultra-high vacuum DC magnetron sputtering system with a magnetic holder. The base pressure was 10^{-7} Torr and the process pressure was 2.5 mTorr. (Ta 2.5 nm/Ru 5 nm) is a seed layer used to promote good <111> texture in Co. In the bottom (Co 5 nm/Ru 0.8 nm/Co 5 nm) trilayer, Co layers of the same thickness are antiferromagnetically coupled to exhibit synthetic antiferromagnet (SAF) behavior. In the top (Co 5 nm/Ru 1.4 nm/Co 10 nm) trilayer, one of the Co layers is thicker such that the antiferromagnetically coupled stack switches as a ferromagnet under the application of an external magnetic field. The film is capped with (Ta 5 nm) to prevent oxidation of the active layers. M-H loops of the bottom and top trilayers are shown in Fig. 2. The pinned layer is antiferromagnetic in the range of magnetic fields tested and the free layer switches in an applied external field of ~80 Oe.

The spin-valve stack was then patterned into a 3×4 array of 700 nm × 600 nm rectangles using a JEOL JBX 5500FS electron beam writer (EBW). A schematic illustrating the major fabrication steps is presented in Fig. 3. The resist used in the lithography process is PMGI/PHOST bilayer. First, Microchem PMGI SF 4S was spin-coated to a thickness of 120 nm and baked at 170 °C for 2 min. Next, 15% PHOST dissolved in PGMEA was spin-coated to a thickness of 680 nm and baked at 170 °C for 2 min. Baking both resists at the same temperature reduces stress and prevents the patterns from popping off during development. Next, a 700 nm wide and 200 μm long line pattern was exposed at a critical dose of 10,000 μC/cm^2; the PHOST was developed by immersing in PGMEA for 15 s. Next,

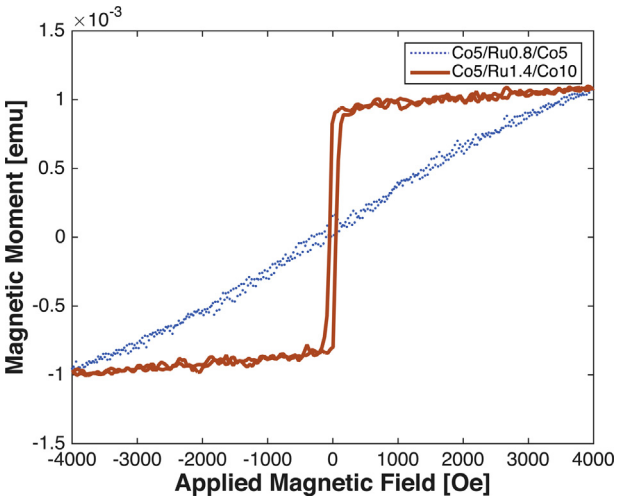

Fig. 2. M-H loops of the bottom and top Co/Ru/Co trilayers used in the spin-valve sensor.

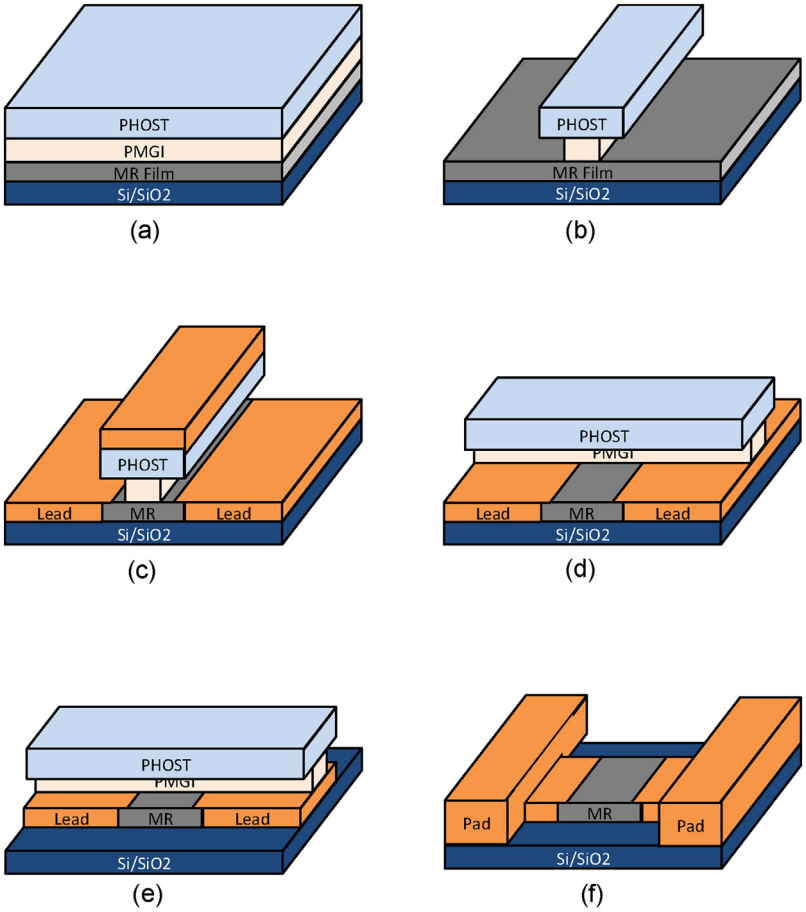

Fig. 3. A diagram of the sensor fabrication sequence: (a) spin-coat PMGI/PHOST bilayer resist; (b) pattern "vertical" lines in PHOST using e-beam lithography, then develop PHOST with PGMEA followed by undercutting PMGI with MF-319; (c) transfer PHOST pattern into spin-valve stack (MR) via argon ion milling followed by sputter deposition of Ta/Cu/Ta leads; (d) strip the resist, spin-coat PMGI/PHOST resist, pattern "horizontal" lines and develop and undercut as in step (b); (e) transfer pattern into spin-valve stack via argon ion-milling; (f) strip the resist and fabricate Ta/Cu contact pads using photolithography.

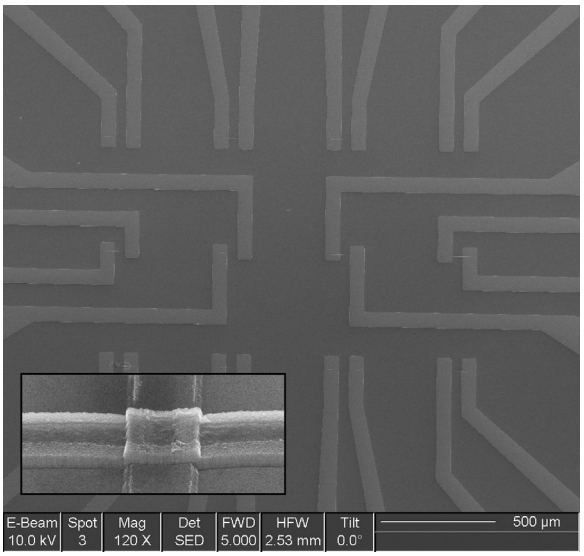

Fig. 4. SEM images of a 3 × 4 sensor array; the inset shows a single MR sensor.

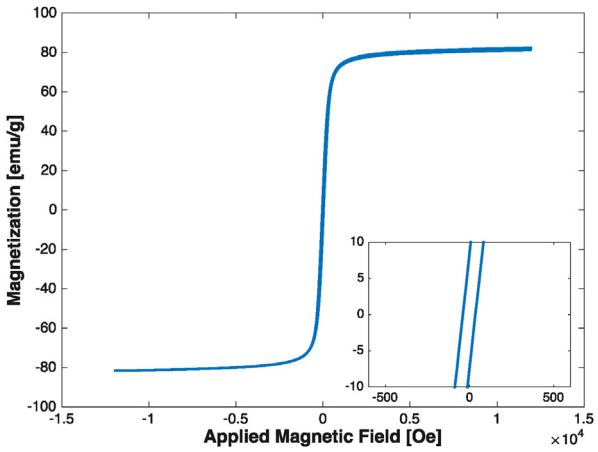

Fig. 5. M-H loops for Fe_3O_4 magnetic particle reporters used in this work. The inset shows the M-H loop between −500 Oe to 500 Oe.

the PMGI was undercut approximately 180 nm deep by immersing in MF-319 for 60 s. The undercut is required to improve the contact between the sensor and the leads. Next, the pattern was transferred into the MR film via argon ion milling. Next, the leads consisting of Ta(2.5 nm)/Cu(50 nm)/Ta(10 nm) were sputter deposited with the gun angles set at 45° with chuck rotation. The top Ta layer is required to enable undercutting of PMGI in the next lithography step because MF-319 etches Cu. Next, the resist was stripped off by immersing in acetone with sonication. Next, the lithography process was repeated with the line pattern printed orthogonal to the first. Next, the pattern was transferred into the MR and leads film via argon ion milling. Next, the resist was stripped off by immersing in acetone with sonication. Next, the pad patterns were created using photolithography with an LOR/AZ1512 bilayer. The contact pads, Ta(10 nm)/Cu(100 nm), were deposited by sputtering without rotation; the guns were set at 45° and the chuck was oriented such that the film was deposited orthogonal to the length of the leads. The sensor array was complete after a final lift-off in acetone with sonication. An SEM image of a 12-sensor array is shown in Fig. 4, and the inset shows a single rectangular sensor.

2.3. Corrosion test

The sensors were coated with a 100 nm pinhole-free layer of Al_2O_3 to prevent corrosion, and the coating also serves as a modifiable surface for attaching bio-functional molecules [21]. The Al_2O_3 layer was reactively sputtered using an Al target at 5 mTorr in a mixture of Ar (35 sccm)/O_2 (6 sccm) with 100 W DC power and 10 W RF bias. The presence or absence of pinholes was evaluated by electrochemical deposition of copper onto Al_2O_3 coated electrodes (70 nm Cu) fabricated on Si wafers (1 to 10 ohm-cm). The electrolyte used was 0.1 M $CuSO_4{}^*5H_2O$ in water. The reference electrode was a 1 mm-diameter copper wire, the counter electrode was a platinum mesh, and the working electrode was the alumina-coated sample. A potential of −300 mV was applied to electrodeposit Cu onto the sample. The growth of mushroom-like Cu deposits across the surface of the sample is an indirect indication of the presence of pinholes [21]. SEM imaging showed no Cu deposits, which confirmed that the alumina coating was pinhole free. The as-deposited 100 nm thick alumina on the sensor array showed no change in resistance when probed with 1 mA current while immersed in phosphate-buffer-saline (PBS) solution for at least 12 h.

2.4. Magnetic labels

Fe_3O_4 magnetic reporter nanoparticles (diameter ~ 500 nm as measured by SEM) used for sensor testing were synthesized following a protocol reported by Li and co-workers with minor modifications [22]. A 65-mL pressure vessel was first charged with iron chloride hexahydrate ($FeCl_3.6H_2O$, 4.08 g) in 30 mL of ethylene glycol followed by the addition of sodium acetate (2.7 g). The solution was then stirred for 30 min, after which polyethylene glycol (1.0 g) and 20 mL of ethylene glycol were added. The flask was sealed using a Teflon cap and stirred at 188 °C for 21 h. The solution was then cooled to room temperature to obtain a black precipitate. The particles were washed using repeated cycles of magnetic separation and alternating re-dispersion in ethanol and water. Fig. 5 shows the hysteresis loop of the as-synthesized, dried Fe_3O_4 powder measured using a vibrating sample magnetometer (VSM); the magnetization was confirmed to be 80 emu/g. To ensure thorough dispersion of the Fe_3O_4 nanoparticles in aqueous media, the as-synthesized nanoparticles were further functionalized with polyethylenimine (PEI). Fe_3O_4 nanoparticles (10 mg) were sonicated for at least 30 min in water (20 mL), followed by the addition of PEI solution (1 mg, 10 mL). The mixture was incubated on a rocker at 70 rpm for 2 h. Subsequently, excess PEI was removed by three cycles of water dispersion and magnetic separation. The final product was re-dispersed in water.

3. Results and discussion

3.1. Sensor performance

A 0.2 mA DC current was used for the resistance measurement while applying an external magnetic field. The applied field utilized was a triangle wave swept from +400 Oe to −400 Oe and back to +400 Oe at a frequency of 0.05 Hz. It took 30 s to probe a single sensor. The ΔR-H loop of a typical sensor with 152 Ω base resistance is shown in Fig. 6. During the measurement, only the free layer was switched and the change of resistance was ~0.25 Ω. Although the magnetoresistive response (ΔR/R) of this spin-valve film was only 2%, the step-like change in the resistance used for particle detection was easily resolvable without any signal processing. The sensor response for many consecutive measurements showed that the switching field reliably fell within ± 10 Oe.

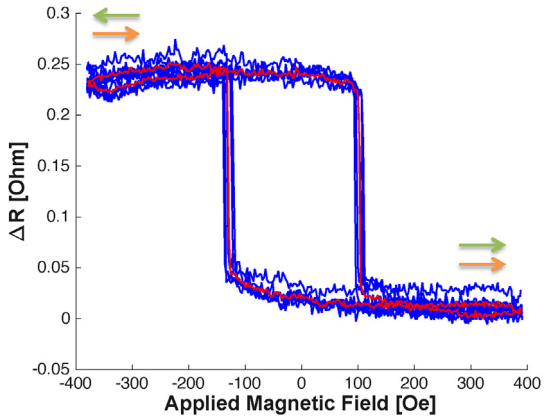

Fig. 6. ΔR-H loop of a typical sensor with 152 Ω base resistance.

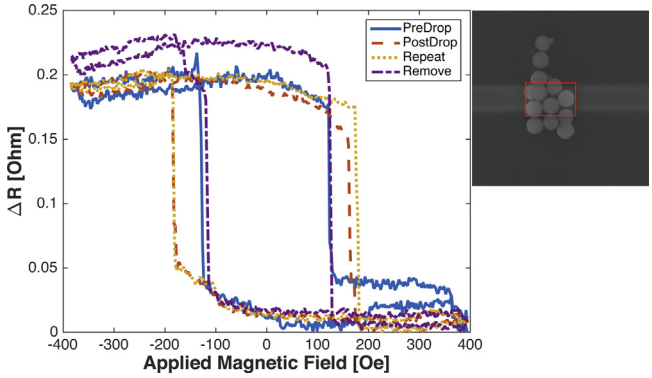

Fig. 7. ΔR-H loop for a sensor with and without magnetic particles. Four sets of data are shown: "PreDrop" is the sensor behavior prior to adding nanoparticles; "PostDrop" and "Repeat" is the sensor behavior in the presence of nanoparticles as shown in the SEM image; "Remove" is the sensor behavior after the removal of nanoparticles. The red box in the SEM image outlines the sensor area. (For interpretation of the references to colour in this figure legend, the reader is referred to the web version of this article.)

3.2. Detection of magnetic nanoparticles

To investigate the sensor performance in the presence of MNPs, 5 μL of a suspension of 500 nm Fe_3O_4 nanoparticles in DI water at a concentration of 0.1 mg/ml was pipetted onto the alumina-coated sensor. After the mixture dried on the alumina surface, SEM was used to check the position of the nanoparticles. Aggregation of MNPs was observed, as shown in the inset to Fig. 7. The aggregation might happen during the synthesis process, re-dispersion, or during drying because of the remnant magnetization. When larger clusters of MNPs are formed, they are more attracted to the magnetic sensors due to stray fields generated by the sensors (even if not energized), thus having a better chance to land on the sensors. Fig. 7 shows the ΔR-H loop of one sensor under 4 consecutive conditions: 1) before applying the particle suspension; 2) after drying and the observation of MNPs; 3) after removing the sensor array from the test station and putting it back; 4) after wiping the MNPs off of the sensor. Before the addition of MNPs, the switching field positions of the sensor were at −128 Oe and +126 Oe. After landing 10 MNPs on the sensor, the switching field positions shifted to −181 Oe and 179 Oe. The switching field positions remained the same after removing and reloading the sensor into the test system. Finally, after wiping the MNPs off the sensor, the switching field positions returned to their original state.

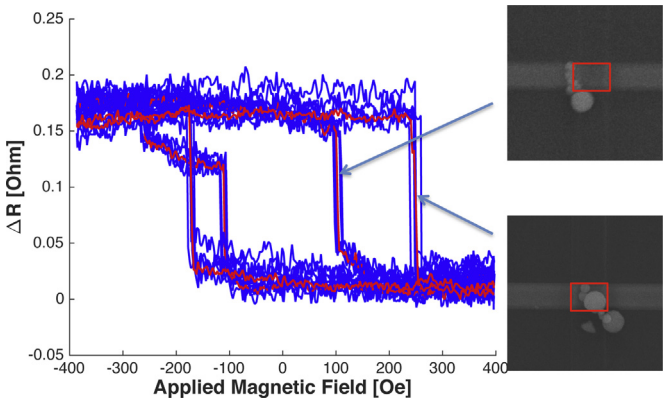

Fig. 9. ΔR-H loops and top-down SEM images of the same sensor before and after particle manipulation. The red line represents the average of 5 consecutive measurements (blue lines). The sensor area (700 × 600 nm^2) is highlighted by red boxes. (For interpretation of the references to colour in this figure legend, the reader is referred to the web version of this article.)

3.3. Detection of single magnetic nanoparticles

An ultra-sharp tungsten tip (TEM sample extraction probe) installed in the FEI 235 Dual-Beam Focused Ion-beam System (FIB) was used to position one MNP over an imitation sensor surface as illustrated in Fig. 8. This process was used to artificially position a single MNP above a sensor surface.

The ΔR-H loops for the sensor with and without MNPs are shown in Fig. 9. The switching field positions were approximately +100 Oe and −110 Oe when there was no MNP above the sensor as shown in the upper right inset of Fig. 9. Then one MNP was artificially moved onto the sensor using the FIB as shown in the bottom right inset of Fig. 9. The presence of the artificially placed MNP above the sensor changed the switching fields to approximately +260 Oe and −170 Oe. There was significant distinction in

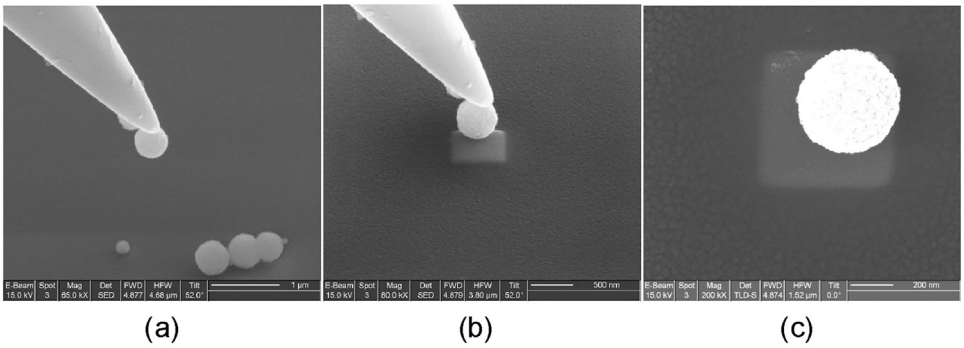

Fig. 8. SEM micrographs demonstrating nanoparticle manipulation: a) picking up a MNP with a tungsten probe; b) placing the MNP on the sensor surface; and c) top-down view after retracting the probe.

the switching fields of a single MNP in proximity to the sensor versus a single MNP in proximity plus a single MNP above the sensor.

4. Conclusions

A spin-valve structure incorporating antiferromagnetically coupled Co/Ru/Co trilayers was developed, and the fabricated MR sensor demonstrated the detection of ten 500 nm MNPs as well as a single 500 nm MNP. The sensing scheme provides a digital signal reporting the presence of a single MNP. This strategy might be effective in the detection of ultra-low concentrations of biomolecules (biomarkers) that are expressed only when the disease is present. The ultimate goal of this project is the ultrasensitive detection of NPM-ALK fusion protein that is expressed in Anaplastic large cell lymphoma (ALCL) the most common T-cell lymphoma in children and young adults [23–25]. The sensors are inexpensive to manufacture and can be arrayed to increase the effective detection area and/or multiplex capabilities. Significantly, the reader electronics, which are basically a current source, Helmholtz coil and voltmeter, can be inexpensively packaged into a portable or mobile system.

Acknowledgments

This work was supported by the Cancer Prevention Research Institute of Texas (Grant No. RP150343), the National Science Foundation (Grants CBET-0932971 and ECCS-1508845), and the Robert A. Welch Foundation (Grant No. E-1320). Additional support by the Center for Integrated Bio and Nano Systems and the Texas Center for Superconductivity at the University of Houston is gratefully acknowledged.

References

[1] D.R. Baselt, G.U. Lee, M. Natesan, S.W. Metzger, P.E. Sheehan, R.J. Colton, A biosensor based on magnetoresistance technology, Biosens. Bioelectron. 13 (7) (1998) 731–739.
[2] J. Schotter, P.B. Kamp, A. Becker, A. Puhler, D. Brinkmann, Willi Schepper, H. Bruckl, G. Reiss, A biochip based on magnetoresistive sensors, IEEE Trans. Magn. 38 (5) (2002) 3365–3367.
[3] J. Llandro, J.J. Palfreyman, A. Ionescu, C.H.W. Barnes, Magnetic biosensor technologies for medical applications: a review, Med. Biol. Eng. Comput. 48 (10) (2010) 977–998.
[4] D.L. Graham, H.A. Ferreira, P.P. Freitas, Magnetoresistive-based biosensors and biochips, Trends Biotechnol. 22 (9) (2004) 455–462.
[5] J. Schotter, P.-B. Kamp, A. Becker, A. Pühler, G. Reiss, H. Brückl, Comparison of a prototype magnetoresistive biosensor to standard fluorescent DNA detection, Biosens. Bioelectron. 19 (10) (2004) 1149–1156.
[6] C.R. Tamanaha, S.P. Mulvaney, J.C. Rife, L.J. Whitman, Magnetic labeling, detection, and system integration, Biosens. Bioelectron. 24 (1) (2008) 1–13.
[7] S.X. Wang, G. Li, Advances in giant magnetoresistance biosensors with magnetic nanoparticle tags: review and outlook, IEEE Trans. Magn. 44 (7) (2008) 1687–1702.
[8] J. Choi, A.W. Gani, D.J.B. Bechstein, J.-R. Lee, P.J. Utz, S.X. Wang, Portable, one-step, and rapid GMR biosensor platform with smartphone interface, Biosens. Bioelectron. 85 (2016) 1–7.
[9] D.H. Blohm, A. Guiseppi-Elie, New developments in microarray technology, Curr. Opin. Biotechnol. 12 (1) (2001) 41–47.
[10] G. Li, S. Sun, R.J. Wilson, R.L. White, N. Pourmand, S.X. Wang, Spin valve sensors for ultrasensitive detection of superparamagnetic nanoparticles for biological applications, Sens. Actuat. A: Phys. 126 (1) (2006) 98–106.
[11] M.M. Miller, G.A. Prinz, S.-F. Cheng, S. Bounnak, Detection of a micron-sized magnetic sphere using a ring-shaped anisotropic magnetoresistance-based sensor: a model for a magnetoresistance-based biosensor, Appl. Phys. Lett. 81 (12) (2002) 2211–2213.
[12] H.A. Ferreira, D.L. Graham, P.P. Freitas, J.M.S. Cabral, Biodetection using magnetically labeled biomolecules and arrays of spin valve sensors, J. Appl. Phys. 93 (10) (2003) 7281–7286.
[13] B. Dieny, Giant magnetoresistance in spin-valve multilayers, J. Magn. Magn. Mater. 136 (3) (1994) 335–359.
[14] P.P. Freitas, R. Ferreira, S. Cardoso, F. Cardoso, Magnetoresistive sensors, J. Phys.: Condens. Matter 19 (16) (2007) 165221.
[15] D.A. Hall, R.S. Gaster, T. Lin, S.J. Osterfeld, S. Han, B. Murmann, S.X. Wang, GMR biosensor arrays: a system perspective, Biosens. Bioelectron. 25 (9) (2010) 2051–2057.
[16] W. Wang, Y. Wang, L. Tu, Y. Feng, T. Klein, J.-P. Wang, Magnetoresistive performance and comparison of supermagnetic nanoparticles on giant magnetoresistive sensor-based detection system, Sci. Rep. 4 (2014) 5716.
[17] P.I. Nikitin, P.M. Vetoshko, T.I. Ksenevich, New type of biosensor based on magnetic nanoparticle detection, J. Magn. Magn. Mater. 311 (1) (2007) 445–449.
[18] K.-M.H. Lenssen, A.E.T. Kuiper, J.J. Van den Broek, R.A.F. Van der Rijt, A. Van Loon, Sensor properties of a robust giant magnetoresistance material system at elevated temperatures, J. Appl. Phys. 87 (2000) 6665–6667.
[19] J.L. Leal, M.H. Kryder, Spin valves exchange biased by Co/Ru/Co synthetic antiferromagnets, J. Appl. Phys. 83 (7) (1998) 3720–3723.
[20] S.S.P. Parkin, N. More, K.P. Roche, Oscillations in exchange coupling and magnetoresistance in metallic superlattice structures: co/Ru, Co/Cr, and Fe/Cr, Phys. Rev. Lett. 64 (19) (1990) 2304.
[21] J. Litvinov, Y.-J. Wang, J. George, P. Chinwangso, S. Brankovic, R.C. Willson, D. Litvinov, Development of pinhole-free amorphous aluminum oxide protective layers for biomedical device applications, Surf. Coat. Technol. 224 (2013) 101–108.
[22] H. Deng, X. Li, Q. Peng, X. Wang, J. Chen, Y. Li, Monodisperse magnetic single-crystal ferrite microspheres, Angew. Chem. Int. Ed. 44 (18) (2005) 2782–2785.
[23] E. Grande, M.V. Bolos, E. Arriola, Targeting oncogenic ALK: a promising strategy for cancer treatment, Mol. Cancer Ther. 10 (2011) 569–579.
[24] C. Damm-Welk, L. Mussolin, M. Zimmermann, M. Pillon, W. Klapper, I. Oschlies, E. e. d'Amor, A. Reiter, W. Woessmann, A. Rosolen, Early assessment of minimal residual disease identifies patients as very high relapse risk in NPM-ALK-positive anaplastic large-cell lymphoma, Blood 123 (2014) 334–337.
[25] S. Perkins, D. Pickering, E. Lowe, D. Zwick, M. Abromowitch, G. Davenport, M. Cairo, W. Sanger, Childhood anaplastic large cell lymphoma has a high incidence of ALK gene rearrangement as determined by immunohistochemical staining and fluorescent in situ hybridisation: a genetic and pathological correlation, Br. J. Haematol. 131 (2005) 624–627.

Biographies

Dr. Wenlan Qiu is a postdoctoral researcher at the Center for Integrated Bio and Nano Systems at the University of Houston. Dr. Qiu obtained her PhD from Materials Science and Engineering program at the University of Houston where she developed a unique magnetic device patterning technology using patterned gettering layers to locally convert magnetic oxides and oxide multilayers into nanoscale magnetic device patterns. Currently, Dr. Qiu's primary research focus is the development of magnetic materials and device patterning techniques for magnetic sensor arrays.

Dr. Long Chang is a Research Assistant Professor of Electrical & Computer Engineering at the University of Houston and Manager at the University of Houston Nanofabrication Facility. He obtained his PhD in Electrical and Computer Engineering at the University of Houston in 2011 specializing in magnetic recording technology and precision instrument design. He has extensive experience with scientific instrument engineering, nanofabrication process development, maintaining/modifying/upgrading nanofabrication instruments, and software engineering.

Dr. Yu-Chi Liang graduated with a PhD in Chemical Engineering from the University of Houston where he has made major contributions to the magnetic biosensor technology. His work has laid the foundation for the results presented in this manuscript. He currently serves at the Data Engineer & Project Lead at Western Digital Corporation.

Dr. Julia Litvinov is a NIEHS postdoctoral fellow at the University of Texas Medical Branch at Galveston, TX. She obtained her PhD in Biomedical Engineering from the University of Houston where she developed corrosion protection and functionalization coatings for the magnetic sensor arrays. Dr. Litvinov currently specializes in development and implementation of antibody screening assays for medical diagnostics applications, validation of molecular assays in clinical samples and development of pathogen/biomarker detection in microfluidic assays.

Dr. Jing Guo is a postdoctoral fellow at the Center for Integrated Bio and Nano Systems at the University of Houston. She obtained her PhD in Electrical Engineering from the University of Kentucky and BS in Physics from Wuhan University. Her expertise is in high precision device patterning using electron beam lithography.

Dr. Yi-Ting Chen is a postdoctoral fellow in the Department of Chemistry at the University of Houston. She obtained her PhD in Chemistry from the University of Houston and BS in Chemistry from National Taiwan Normal University. Her research is focused on the fabrication of magnetic nanoparticles. Dr. Chen developed Fe_3O_4 magnetic nanoparticles that have been used for proof-of-concept demonstration of particle detection presented in this work.

Dr. Binh Vu is a Research Engineer at the University of Houston. He obtained his PhD in Chemical Engineering from the University of Houston. Dr. Vu has a strong multidisciplinary background and deep expertise in instrument engineering and integration for diagnostics and detection both in academia and in private industry where he developed a point-of-care Lab-on-Chip device, called Gene-RADAR®. Gene-RADAR® has recently won the grand prize in the Nokia Sensing X-Challenge and has been widely featured by major news organizations for its potential applications.

Dr. Katerina Kourentzi is a Research Associate Professor of Chemical & Biomolecular Engineering at the University of Houston with long experience in point-of-care detection methods and antibody-based biosensor technologies. Dr. Kourentzi obtained her PhD and MS degrees in Chemical Engineering from the University of Houston. She has over 40 publications in peer-reviewed journals.

Dr. Shoujun Xu is an Associate Professor of Chemistry at the University of Houston. He obtained his PhD in Chemistry from the Johns Hopkins University and received postdoctoral training at Caltech and the University of California at Berkeley. His expertise includes magnetic detection, atomic magnetometry, molecular imaging, magnetic resonance imaging, spectroscopy and technology development. Dr. Xu invented the force-induced remnant magnetization spectroscopy (FIRMS) technique. Its high force resolution has enabled a wide range of applications in biochemical research. Multiple papers have been published in prestigious scientific journals, and several patents have been either awarded or are pending.

Dr. T. Randall Lee is Cullen Distinguished University Chair of Chemistry at the University of Houston. He obtained his PhD from Harvard and received postdoctoral training from Caltech. Dr. Lee's research centers around the use of synthesis be it organic, inorganic, organometallic, or solid-state to develop new functional interfaces and nanoparticles for technological applications. Dr. Lee has over 240 publications in peer-review journals.

Dr. Youli Zu joined the Department of Pathology and Genomic Medicine at Houston Methodist Hospital in 2004, where he currently serves as the Medical Director of the Hematopathology Section. He is also Professor of Pathology and Laboratory Medicine at the Weill Cornell Medical College of Cornell University. In addition to his clinical responsibilities, Dr. Zu is also the Director of the Cancer Pathology research laboratory at the Houston Methodist Research Institute. Dr. Zu obtained his PhD from Kyoto University Graduate School of Medicine and MD from Jilin Medical College.

Dr. Richard Willson is Huffington-Woestemeyer Distinguished Professor of Chemical and Biomolecular Engineering, Biochemistry, and Biomedical Engineering at the University of Houston. He obtained his PhD and MS degrees from MIT and Caltech, respectively. Dr. Willson is a Senior Affiliate of the Houston Methodist Research Institute at The Methodist Hospital and a member of the SCBMB program at the Baylor College of Medicine. His academic training at Caltech and MIT was in Chemical and Biochemical engineering; he was then a post-doctoral researcher in Biology at MIT. Dr. Willson is a fellow of the AAAS, ACS, AIMBE and NAI, and former Theme Leader for Diagnostics of the US NIH Western Regional Center of Excellence in Biodefense and Emerging Infectious Diseases. His lab has developed several point-of-care diagnostic technologies especially tests using novel reporter particles (including novel lateral-flow methods and optical instruments) and has also transferred several technologies to industry for further development.

Dr. Dmitri Litvinov is a John and Rebecca Moores Professor of Electrical & Computer Engineering, Chemical & Biomolecular Engineering, Materials Science & Engineering, and Chemistry at the University of Houston. He obtained his PhD from the University of Michigan in Ann Arbor, MI. Prof. Litvinov's expertise and research focus are in design and fabrication of magnetic materials and devices at the nanoscale with over 130 publications in peer-review journals and 25 issued patents with Seagate Technology where he used to work as a Research Staff Member before joining the academia. He has developed and implemented a number of novel nanomagnetic device concepts in commercial systems. He is a member of the National Academy of Inventors.